PHYSICAL REVIEW B **84**, 174406 (2011)

Photoemission electron microscopy of three-dimensional magnetization configurations in core-shell nanostructures

Judith Kimling,[1,*] Florian Kronast,[2,†] Stephan Martens,[1] Tim Böhnert,[1] Michael Martens,[1] Julia Herrero-Albillos,[2,‡] Logane Tati-Bismaths,[2] Ulrich Merkt,[1] Kornelius Nielsch,[1] and Guido Meier[1]

[1]*Institut für Angewandte Physik und Zentrum für Mikrostrukturforschung Hamburg, Universität Hamburg, Jungiusstrasse 11, D-20355 Hamburg, Germany*

[2]*Helmholtz-Zentrum Berlin für Materialien und Energie GmbH, Albert-Einstein-Strasse 15, D-12489 Berlin, Germany*

(Received 5 April 2011; revised manuscript received 4 July 2011; published 9 November 2011)

We present a photoemission electron microscopy method that combines magnetic imaging of the surface and of the inner magnetization in three-dimensional core-shell nanostructures. The structure investigated consists of a cylindrical nickel core that is completely surrounded by a shell of iron oxide and silicon oxide layers. The method enables one to image the magnetization configuration of the nickel core even though the shell is thicker than the mean-free path of the photoelectrons. Characteristic L_3 and L_2 edges can be observed not only in the yield of the photoelectrons emitted from the surface of the nanostructure but also in its shadow. X-ray magnetic circular dichroism in the electron yield of the x rays absorbed and transmitted by the multilayered nanowire allows for the individual imaging of the magnetization configurations of the iron oxide tube and the nickel core. The method suggests novel approaches for the characterization of the magnetic and material properties of complex three-dimensional nanostructures.

DOI: 10.1103/PhysRevB.84.174406 PACS number(s): 75.75.−c, 68.37.Yz, 81.07.−b

I. INTRODUCTION

A large variety of techniques is available today to visualize the magnetization reversal of microstructures and nanostructures.[1] Which technique is best suited in a particular case depends on the considerations concerning spatial and temporal resolution as well as the complexity of the sample, to mention a few. When element specificity is required, the selection reduces to techniques based on x-ray absorption. Here, the magnetic contrast in ferromagnets and ferrimagnets arises from an asymmetry of the absorption cross sections of atomic core levels for left and right circularly polarized x-ray photons, called x-ray magnetic circular dichroism (XMCD).[2] X-ray magnetic linear dichroism even allows for the study of antiferromagnets.[3] In both cases a spatially resolved magnetic contrast can be obtained from the difference of two intensity measurements (one for each polarization) either of the transmitted x rays as in magnetic transmission x-ray microscopy[4] or of the electron yield as in photoemission electron microscopy (PEEM).[5,6] While transmission x-ray microscopy averages over the volume of the traversed sample, the sampling depth of PEEM is determined by the mean free path of the photoelectrons, making it a surface-sensitive technique.[2] Both methods are being improved constantly. Nowadays, they provide time resolution in the picosecond range[7–9] and a lateral resolution down to a few nanometers.[10,11] It has been shown recently that standing-wave excitation can add dimensionality to PEEM.[12,13] In particular, sampling interfaces or nanoobjects with standing waves can provide additional depth resolution down to a few Ångstroms. However, due to the period of the standing wave and the mean free path of the photoelectrons the sampling depth is limited to a few nanometers.

The resonant character of x-ray excitation opens unique possibilities for the study of core-shell nanoparticles, where one challenge lies in separating the magnetic contributions of the individual components.[14] In this work we present a method based on PEEM combining surface and bulk sensitive XMCD contrast. Extending the conventional PEEM imaging with a transmission experiment, it is possible to record magnetic information originating both from the surface and from the internal components of a nanostructure and to separate those two contributions. To prove that magnetic information can be obtained from regions below the sampling depth of photoelectrons, we employ cylindrical nickel nanowires surrounded by an approximately 27 nm thick shell of iron oxide and silicon dioxide. The individual magnetization states of the nickel core and the surrounding iron oxide tube are successfully imaged.

II. EXPERIMENTAL DETAILS

The multilayered core-shell nanowires studied in this work are synthesized by filling the hexagonally ordered pores of an alumina membrane with different materials and with different techniques.[15] In a first step, the pores are coated with SiO_2(5 nm)/Fe_2O_3(12 nm)/SiO_2(10 nm) by atomic layer deposition. Then the tubes are filled with nickel by electrochemical deposition. The nickel core has a diameter of about 100 nm that is determined by the pore diameter and the thickness of the shell layers. In the next step the template is removed by selective chemical etching in chromic acid. After filtration the individual core-shell wires are suspended in water. For PEEM imaging the solution is dripped onto a silicon wafer with a specific resistivity of about 10 Ωcm and left to dry in a magnetic field to align the wires in parallel. Before the experiment the Fe_2O_3 is reduced to Fe_3O_4 by annealing the sample in an argon-hydrogen atmosphere at 350 °C for 3 hours. The sample holder used for PEEM imaging allows for the application of a uniaxial in-plane field up to 200 mT (Ref. 16). PEEM imaging was performed at the undulator beamline UE49 PGM of the synchrotron light source BESSY II in Berlin, Germany. The beamline provides photons in the range from 100 to 1800 eV with an energy resolution $E/\Delta E = 10\,000$ at

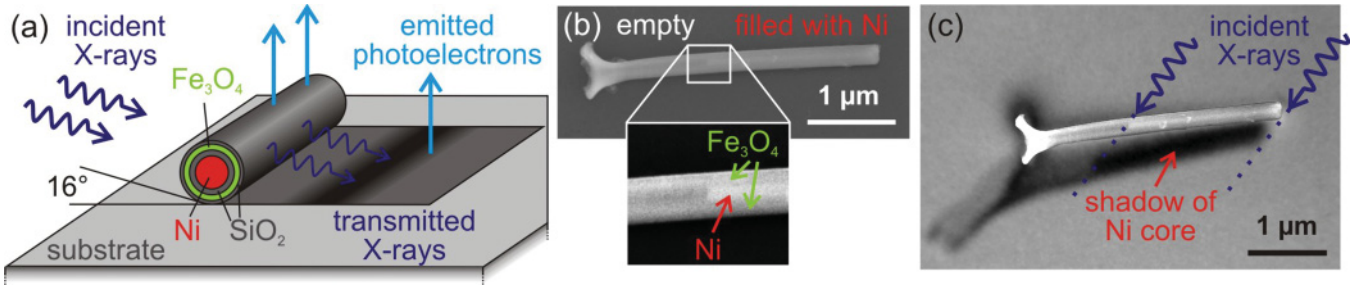

FIG. 1. (Color) (a) Schematic of a core-shell wire during PEEM imaging. (b) Scanning electron micrograph of an iron oxide tube partially filled with a nickel core. The blow up shows the transition from the empty tube (left) to the nickel core (right) that appears bright. (c) Cutout of a scanning electron micrograph combined with a PEEM image recorded at the nickel edge. The absorption of the nickel core can be distinguished in the shadow of the wire.

700 eV and full polarization control. The schematic of a core-shell wire on a silicon wafer exposed to an x-ray beam is shown in Fig. 1(a). The incident x rays hit the sample surface under an angle of 16°. Photoelectrons are emitted from the surface of the wire and the substrate. Details about the PEEM setup are described elsewhere.[16] A scanning electron micrograph of the core-shell nanowire that we have investigated is shown in Fig. 1(b). It reveals that the iron oxide tube is only partially filled with a nickel core. The nickel core appears bright due to the increased scattering of the secondary electrons. Figure 1(c) is the overlay of a scanning electron micrograph and a PEEM image recorded at the nickel edge. The nickel core can clearly be distinguished in the shadow of the structure. To observe both this shadow and the XMCD contrast caused by the magnetization components along the wire axis, an angle of about 45° between the in-plane projection of the incident x rays and the wire axis was chosen for imaging the magnetization reversal. At 90° the shadow would be larger, but only the magnetization components perpendicular to the wire axis could be mapped, while at 0° the XMCD contrast would be most sensitive to the magnetic moments aligned along the wire axis, but no shadow of the nickel core could be observed.

III. RESULTS AND DISCUSSION

Photoemission spectra from selected areas marked in the inserted PEEM image are shown in Fig. 2(a). The electron yield measured on the wire (curve A) gives a spectrum that is proportional to the x-ray absorption coefficient of the iron oxide. The absorbed x rays cause transitions into unoccupied 3*d* levels leading to iron-specific resonance peaks. The step-like background is caused by transitions into continuum states. For iron and nickel the electron sampling depth is about 5 nm (Ref. 17). Due to this surface sensitivity the nickel core does not contribute to the signal measured on the nanowire as it is evidenced by the blue curve (A) in Fig. 2(a). The x-ray absorption length is about one order of magnitude higher than the electron sampling depth. Some x-ray photons are transmitted through the nanostructure and excite photoelectrons in the substrate. The yield of these electrons emitted from the shadow area of the wire is also shown in Fig. 2(a). While the L_3 and L_2 edges of iron can be observed both on the wire (curve A) and in the entire shadow region (curves B and C), the nickel L_3 and L_2 edges are observed only in the shadow of the nickel core (curve C). The spectra recorded in the shadow are inverted with respect to the photoemission spectrum recorded on the wire since they are transmission spectra. Figure 2(b) illustrates the two areas in the shadow where the element-specific absorption lines and thereby the XMCD contrast of the respective materials can be observed.

Our experiment demonstrates that combining the conventional surface sensitive PEEM microspectroscopy with a transmission experiment, element-specific magnetic information of complex three-dimensional nanostructures can be obtained,

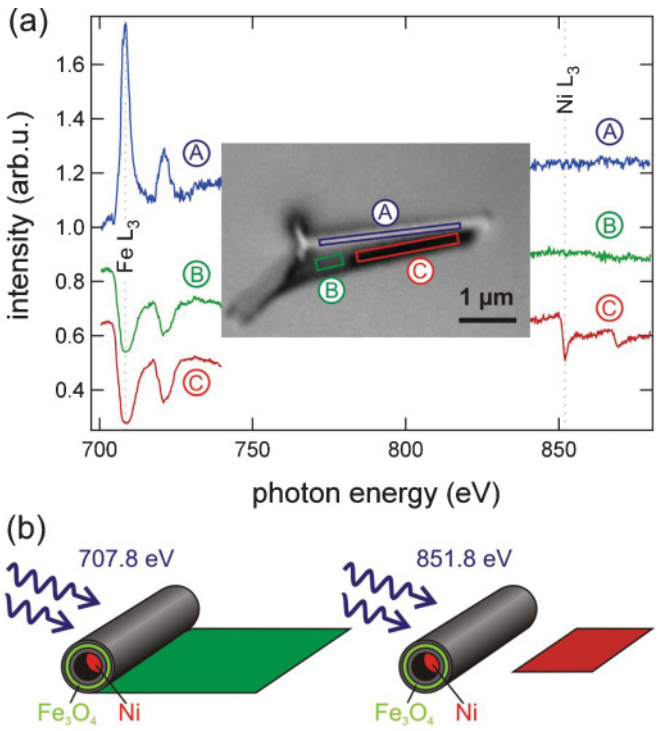

FIG. 2. (Color) (a) Photoemission spectra recorded on the wire (A, blue), in the shadow of the empty tube (B, green), and in the shadow of the nickel core (C, red). The respective regions are marked in the PEEM image shown in the middle. The red curves are shifted for clarity by −0.3. Note, that no absorption edges of the silicon substrate contribute in the energy range shown. (b) Schematic of a partially filled core-shell wire exposed to x rays of different photon energies. At 707.8 eV (Fe L_3 edge) XMCD contrast revealing the magnetic configuration of the iron oxide tube is obtained in the entire shadow region (green), while at 851.8 eV (Ni L_3 edge) magnetic contrast is only obtained in the shadow of the nickel core (red).

even though components are buried below the sampling depth of photoelectrons.

To image the magnetic configuration of the iron oxide tube and the nickel core, XMCD images are recorded at both the iron and the nickel L_3 edge. The XMCD images shown in the following figures represent the difference of two PEEM images recorded with circularly polarized x rays of opposite helicity, divided by their sum. Figure 3(a) shows PEEM images of the core-shell wire recorded at the iron L_3 and at the nickel L_3 edge after extraction of the background. The increased absorption by the nickel core is visible in the shadow only at the nickel edge. Figures 3(b) through 3(e) are pairs of differential XMCD images recorded at the respective absorption edges revealing the remanent magnetization configurations of the iron oxide shell (left) and the nickel core (right). The blue and red XMCD contrasts are proportional to the magnetization parallel and antiparallel to the direction of the in-plane projection of the incident x-ray beam, respectively. Thus, these contrasts indicate the magnetization components along the wire axis. The magnetization of the white areas is either zero or aligned normal to the photon wave vector. At the iron edge (707.8 eV) magnetic contrast can be obtained both on the surface of the wire and in its shadow. The contrast in the shadow is inverted as the electron yield from the substrate is proportional to the intensity of the transmitted x rays. At the nickel edge (851.8 eV) magnetic contrast can only be observed in a segment of the shadow. Comparing this area in Figs. 2 and 3 shows that this segment corresponds to the area where the nickel-specific absorption lines are observed in Fig. 2, namely the shadow of the nickel core.

The magnetic configurations shown in the image pairs in Figs. 3(b) through 3(e) are prepared as follows: first the structure is saturated along the wire axis in an external magnetic field. Then a reverse magnetic field is applied before the field is set to zero and XMCD images are taken in remanence.[18] This procedure is repeated for every image pair.[19] The magnitude of the reverse field for the individual image pairs is given in the figure. Figure 3(b) depicts the remanent state after saturation. The magnetizations of the two coaxial nanomagnets are aligned in parallel. In Fig. 3(c) the magnetic contrast of the nickel core remains the same compared to Fig. 3(b), while the XMCD contrast of the electrons emitted from the iron oxide tube increases. Given the direction of incidence of the x rays which is 45° to the wire axis, and given a constant magnetic moment, this means that the magnetization of the tube becomes tilted further away from the wire axis. At the same time the magnetic contrast in the shadow of the tube becomes more inhomogeneous and locally almost vanishes. This could be explained as follows: the x rays causing the XMCD contrast in the shadow probe the magnetization components of the two side walls of the tube. If the magnetization, for example, curls as described in the model of Chong *et al.*,[15] the contributions cancel and the contrast is lost. Figure 3(d) represents the remanent magnetization configurations after applying a magnetic field in the vicinity of the switching field. The feature of the vanishing shadow is observed again on the right end of the tube, where the magnetization has not switched yet. The nickel core also started to reverse its magnetization, and a domain wall can be observed. In Fig. 3(e) the reverse field applied is high enough to completely switch the magnetization of the iron oxide tube and the nickel core.

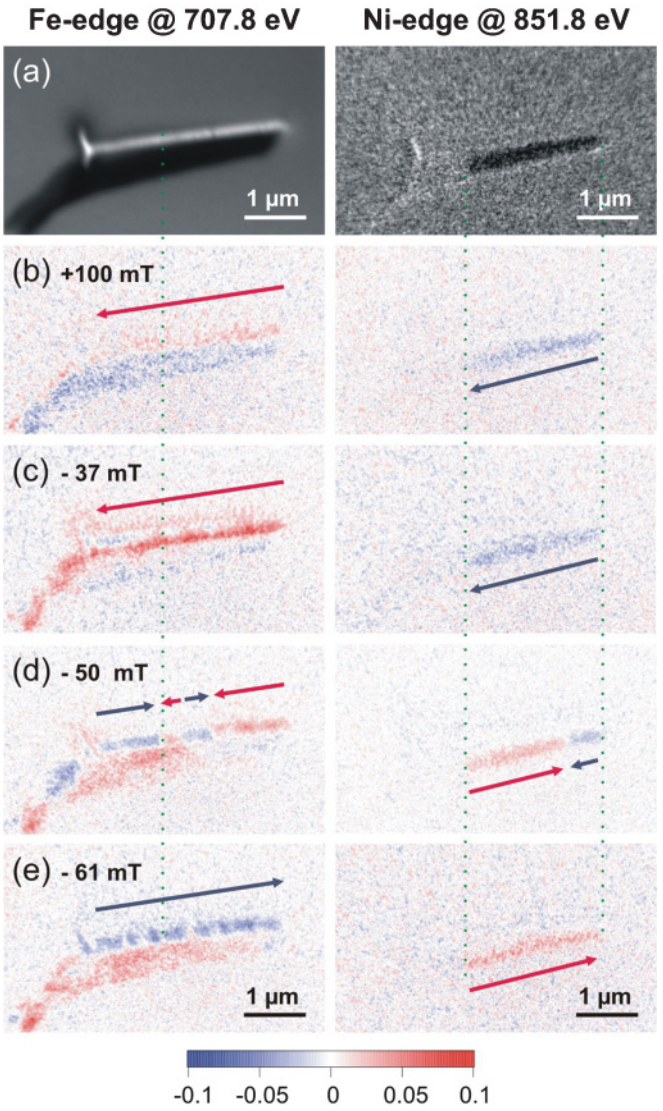

FIG. 3. (Color) (a) PEEM images of the core-shell wire recorded at the iron L_3 edge and the nickel L_3 edge (background extracted). (b)–(e) Differential XMCD images of the iron oxide tube (left) and the nickel core (right) recorded at the respective absorption edges. The color bar indicates the direction of the magnetic contrast in arbitrary units. The magnetic configurations are imaged in remanence after saturating at (b) −123 mT and (c)–(e) +123 mT and applying the displayed field values. (The values of the magnetic field are estimated from the position of the wire relative to the center of the pole shoes of the sample holder and the coil currents applied. Due to the remanence of the pole shoes we assume an error of approximately 1.4 mT in the displayed field values.) The arrows indicate the magnetization components along the wire axis. The green dotted lines mark the ends of the nickel core.

The remanent magnetization configurations provide a hint at the contrasting magnetic behavior of the iron oxide tube and the nickel core. In nickel the magnetocrystalline anisotropy is low (5 000 J/m^3). Thus, the magnetic easy axis of the core is given by its cylindrical shape and the high aspect ratio, and the magnetic moments remain aligned along the

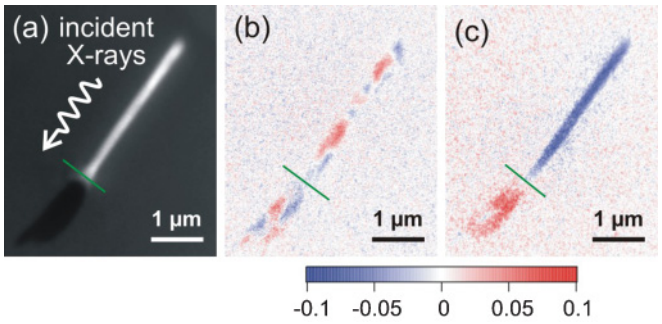

FIG. 4. (Color) (a) PEEM image of the core-shell wire taken at an angle of 0° between wire axis and incident x rays. (b) Differential XMCD image recorded at the iron L_3 edge in zero magnetic field after annealing (as-prepared) and (c) after the first field sweep 120 mT → −120 mT → 0 mT. The blue and red XMCD contrasts represent magnetizations along and antiparallel to the wire axis, respectively. The green lines mark the wire end.

wire axis even though the material is not single-crystalline. Apart from one abrupt contrast change, the magnetization of the nickel core appears homogeneous. This suggests magnetization reversal via domain-wall motion as predicted by micromagnetic simulations.[20] During propagation domain walls can be stopped by defects in the wire serving as pinning sites. The intrinsic anisotropy of the iron oxide tube is determined by an interplay of magnetostatic energy, exchange energy, and magnetocrystalline anisotropy. Since the walls of the tube are only 12 nm thick, the tube is expected to behave as a rolled-up thin film, in which the magnetization tends to align in the plane.[21] The magnetostatic energy associated with surface charges is minimized if the magnetization curls radially around the tube, while the exchange energy favors a parallel alignment of the magnetic moments along the wire axis. A typical magnetic state calculated for ferromagnetic tubes is a uniform magnetization along the axis in the middle part of the tube, and two vortices curling at the ends.[21,22] For the magnetization reversal the propagation of a vortex or a transverse domain wall from one end of the tube to the other is predicted.[21]

Figure 4 depicts PEEM images recorded at an angle of about 0° between the in-plane projection of the incident x-ray beam and wire axis. Figure 4(c) shows the remanent magnetization components along the wire axis after saturation at −120 mT. In agreement with the XMCD image of the comparable state recorded at 45° [Fig. 3(b)] the magnetization is not completely homogeneous, but predominantly aligned in the same direction along the wire axis. Both the images of the remanent states after saturation as well as the other magnetic states shown in Fig. 3 do not clearly evidence an increased rotation of the magnetization at the tube's end away from the wire axis (i.e., the theoretically predicted vortices).

In Figs. 3(c) through 3(e) the magnetization of the tube appears inhomogeneous. This might be attributable to the granularity of the iron oxide tube.[15,23] It has been shown analytically that the intrinsic anisotropy of a nanotube can be tailored by tuning the aspect ratio between radius, thickness, and length of the tube, and even be reduced to zero for soft magnetic materials.[22] In the present tube the contribution of the magnetocrystalline anisotropy of the iron oxide (11 000 J/m^3) to the intrinsic anisotropy of the tube seems to be comparably high. The influence of the magnetocrystalline anisotropy and the random orientation of the grains in the iron oxide tube becomes apparent in the as-prepared magnetization configuration of the tube shown in Fig. 4(b). The term as-prepared refers to the state of the sample after reduction by annealing. Our data point to a discrepancy between theoretical predictions and the actual magnetization reversal process of the iron oxide tube. This indicates that the granular structure of the material should be implemented in the models.

IV. CONCLUSION

We have shown that separate PEEM imaging of the individual layers of core-shell nanostructures is possible, even if a layer is buried deeper than the sampling depth of the photoelectrons. Conventional surface sensitive PEEM is successfully combined with a transmission experiment probing the magnetization of inner components. The method enables one to image the individual magnetization configurations of two coaxial nanomagnets, an iron oxide tube, and an enclosed nickel core. Contributions originating from the surface and from the interior of a nanostructure can be separated, an interesting feature not only for magnetic characterizations but also for material analysis. Due to the limited x-ray transmission, the method is applicable to nanostructures with a maximum thickness of about 300 nm. In principle, it is possible to obtain full three-dimensional magnetic information by tomography.[24] Given the possibility to image in an applied magnetic field up to about 40 mT (Ref. 16), element specificity, a potential lateral resolution of a few nanometers and the option to implement time resolution in the picosecond range, the method opens new avenues for the study of magnetization reversal in complex three-dimensional nanostructures.

ACKNOWLEDGMENTS

The authors thank Yuen Tung Chong for providing the core-shell nanostructures, Peter Lendecke for help with the measurements, and Julien Bachmann and Detlef Görlitz for fruitful discussions. Financial support by the Deutsche Forschungsgemeinschaft via the Sonderforschungsbereich 668 and the Graduiertenkolleg 1286 as well as by the Forschungs- und Wissenschaftsstiftung Hamburg via the Cluster of Excellence Nanospintronics and by the Helmholtz-Zentrum Berlin is gratefully acknowledged.

*judith.kimling@physnet.uni-hamburg.de
†florian.kronast@helmholtz-berlin.de
‡Present addresses: Centro Universitario de la Defensa de Zaragoza, Carretera de Huesca s/n, E-50090 Zaragoza, Spain and Instituto de

Ciencia de Materiales de Aragón and Departamento de Física de la Materia Condensada, CSIC-Universidad de Zaragoza, E-50009 Zaragoza, Spain.

[1]M. R. Freeman and B. C. Choi, Science **294**, 1484 (2001).
[2]J. Stöhr, H. A. Padmore, S. Anders, T. Stammler, and M. R. Scheinfein, Surf. Rev. Lett. **5**, 1297 (1998).
[3]F. Nolting *et al*., Nature (London) **405**, 767 (2000).
[4]P. Fischer, IEEE J. Quantum Electron. **42**, 36 (2006).
[5]A. Locatelli and E. Bauer, J. Phys.: Condens. Matter **20**, 093002 (2008).
[6]C. M. Schneider and G. Schönhense, Rep. Prog. Phys. **65**, R1785 (2002).
[7]T. Kamionka, M. Martens, K. W. Chou, M. Curcic, A. Drews, G. Schütz, T. Tyliszczak, H. Stoll, B. Van Waeyenberge, and G. Meier, Phys. Rev. Lett. **105**, 137204 (2010).
[8]J. Raabe, C. Quitmann, C. H. Back, F. Nolting, S. Johnson, and C. Buehler, Phys. Rev. Lett. **94**, 217204 (2005).
[9]B. Heitkamp, F. Kronast, L. Heyne, H. A. Dürr, W. Eberhardt, S. Landis, and B. Rodmacq, J. Phys. D: Appl. Phys. **41**, 164002 (2008).
[10]W. Chao, J. Kim, S. Rekawa, P. Fischer, and E. H. Anderson, Opt. Express **17**, 17669 (2009).
[11]R. Fink *et al*., J. Electron Spectrosc. Relat. Phenom. **84**, 231 (1997).
[12]F. Kronast *et al*., Appl. Phys. Lett. **93**, 243116 (2008).
[13]A. X. Gray *et al*., Appl. Phys. Lett. **97**, 062503 (2010).
[14]H. A. Dürr *et al*., IEEE Trans. Magn. **45**, 15 (2009).
[15]Y. T. Chong, D. Görlitz, S. Martens, M. Y. E. Yau, S. Allende, J. Bachmann, and K. Nielsch, Adv. Mater. **22**, 2435 (2010); Y. T. Chong (Private communication).
[16]F. Kronast, J. Schlichting, F. Radu, S. K. Mishra, T. Noll, and H. A. Dürr, Surf. Interface Anal. **42**, 1532 (2010).
[17]R. Nakajima, J. Stöhr, and Y. U. Idzerda, Phys. Rev. B **59**, 6421 (1999).
[18]The remanent magnetization configurations might differ from the ones prepared while an external magnetic field is applied. With our method it is possible to perform magnetic imaging in an applied magnetic field up to about 40 mT. This field is too low for imaging the magnetization reversal of the present nanostructure.
[19]In the image pair Fig. 3(d) the differential XMCD image obtained at the nickel edge was replaced by an image with better statistics. In the image shown the magnetic state of the nickel core is the same as in the image replaced. The images were taken during different field cycles with a reverse field of about 50 mT.
[20]R. Hertel and J. Kirschner, Physica B **343**, 206 (2004).
[21]J. Escrig, J. Bachmann, J. Jing, M. Daub, D. Altbir, and K. Nielsch, Phys. Rev. B **77**, 214421 (2008).
[22]A. P. Chen, K. Y. Guslienko, and J. Gonzalez, J. Appl. Phys. **108**, 083920 (2010).
[23]R. Zierold, Z. Wu, J. Biskupek, U. Kaiser, J. Bachmann, C. E. Krill, and K. Nielsch, Adv. Funct. Mater. **21**, 226 (2010).
[24]A. Fraile Rodriguez, A. Kleibert, J. Bansmann, A. Voitkans, L. J. Heyderman, and F. Nolting, Phys. Rev. Lett. **104**, 127201 (2010); By an azimuthal rotation of the sample the absolute value and direction of the magnetic moments can be determined. For this purpose it would be required to image the same magnetic state at several angles between the direction of the incident x rays and the wire axis.